Circular Dichroism and Redox Properties of High Redox Potential Ferredoxins†

Craig T. Przysiecki,‡ Terrance E. Meyer, and Michael A. Cusanovich*
Department of Biochemistry, University of Arizona, Tucson, Arizona 85721
Received September 17, 1984

ABSTRACT: The circular dichroism (CD) spectra of 13 examples of high-potential iron–sulfur proteins (HiPIPs), a class of [4Fe-4S] ferredoxins, have been determined. In contrast to the proposal of Carter [Carter, C. W., Jr. (1977) *J. Biol. Chem. 252*, 7802–7811], no strict correlation between visible CD features and utilization of the $[4Fe\text{-}4S]^{2+}/[4Fe\text{-}4S]^{3+}$ oxidation levels was found. Although most HiPIPs have these features, the model requires their presence in all species. There is also no simple relationship between CD spectral features and the presence of conserved tyrosine-19. In addition, no apparent correlation between CD properties and oxidation–reduction potential could be detected. However, amino acid side chains in close contact to the iron–sulfur cluster appear to be important in modulating spectral and oxidation–reduction properties. In particular, the negative shoulder at 290 nm and negative maximum at 230 nm correlate with the presence of Trp-80 (*Chromatium vinosum* numbering). Two HiPIPs that do not have Trp at this position have positive bands at 290 and 230 nm. These bands in the *Ectothiorhodospira halophila* HiPIPs are apparently associated with Trp-49, which is located on the opposite side of the effective mirror plane of the cluster from Trp-80. The effect of pH on circular dichroism and redox potential in *Thiocapsa roseopersicina* HiPIP, which has a histidine at position 49, is consistent with the interaction of the side chain with the cluster. Despite specific differences in their CD spectra, the various HiPIPs studied show general similarity consistent with structural homology within this class of iron–sulfur proteins.

High-potential iron–sulfur protein (HiPIP)[1] is the trivial name used to designate a class of [4Fe-4S] ferredoxins found in many purple photosynthetic bacteria and at least one halophilic, denitrifying bacterium (Bartsch, 1978; Meyer et al., 1983). The proteins form a single distinct structural class, on the basis of apparent amino acid sequence homology, with four cysteine residues ligating the irons of the single cubane-like [4Fe-4S] cluster (Tedro et al., 1981). As their name suggests, the proteins undergo a reversible one-electron transfer reaction at a characteristically high oxidation–reduction midpoint potential (≥50 mV; Meyer et al., 1983). The exact functional role of HiPIP in anaerobic electron transport is unknown; however, *Chromatium vinosum* HiPIP has been found to be a good electron acceptor for a thiosulfate-oxidizing enzyme isolated and partially purified from that organism (Fukumori & Yamanaka, 1979).

A more widely distributed [4Fe-4S] ferredoxin class from anaerobic bacteria (known by the trivial name bacterial ferredoxin) have very low redox potentials; for example, the potential of the two equivalent clusters in *Peptococcus aerogenes* 2[4Fe-4S] ferredoxin is −427 mV (Stombaugh et al., 1976). On the basis of the similarity of the structures of the reduced cluster of *C. vinosum* HiPIP and the oxidized clusters of *P. aerogenes* ferredoxin (Carter et al., 1972) as well as studies with cluster analogues (Herskovitz et al., 1972), the drastic difference in oxidation–reduction potentials has been reconciled by the proposal that the two proteins use different oxidation levels of the cluster, the now well-established three-state hypothesis of Carter and co-workers (1972). The cluster oxidation levels used are 3+, 2+, and 1+, each differing by one electron, and represent the net charge of the cluster excluding the cysteinyl sulfur charge contributions. In terms of formal iron valences only, the 3+, 2+, and 1+ states correspond to $[Fe(III)_3Fe(II)_1]$, $[Fe(III)_2Fe(II)_2]$, and $[Fe(III)_1Fe(II)_3]$, respectively (Herskovitz et al., 1972). In *C. vinosum* HiPIP (and other HiPIP examples), the cluster is restricted to the 3+ and 2+ oxidation levels, under native conditions, being oxidized from the diamagnetic, 2+ level, to the paramagnetic ($g_{av} > 2$) 3+ level. In contrast, the clusters in *P. aerogenes* are reduced from the 2+ level to the paramagnetic ($g_{av} < 2$) 1+ oxidation level. Differences in the cluster binding cavities are thought to restrict the [4Fe-4S] clusters in these proteins to their respective oxidation levels. In favor of this hypothesis, HiPIP can be reduced to the normally unobtainable 1+ oxidation level, termed superreduced HiPIP, upon unfolding of the protein in 80% Me_2SO (Cammack, 1973). The protein structural features responsible for this thermodynamic prevention of superreduction in native HiPIP are not known in detail [cf. Sweeney & Rabinowitz (1980)]. Nevertheless, it has been suggested that differential exposure of the cluster to solvent, geometric or electronic distortion of the cluster, and stabilization of cluster charge by NH···S hydrogen bonds may be involved in determining the [4Fe-4S] cluster redox states used by a protein [cf. Sweeney & Rabinowitz (1980) and references cited therein].

Carter (1977b) has proposed that different cluster environments in the two types of [4Fe-4S] ferredoxins may arise from tyrosine side chain (the strictly conserved Tyr-19 in HiPIP) interactions with an inorganic sulfur of the cluster. These tryosine/cluster interactions within *C. vinosum* HiPIP and *P. aerogenes* 2[4Fe-4S] ferredoxin are from opposite sides of an effective mirror plane of the cluster and, along with other peptide interactions, place the clusters into diastereomeric environments. A pair of bands of opposite ellipticity in the visible CD spectrum of one reduced HiPIP, *C. vinosum*

† This work was supported by a grant from the National Institutes of Health (GM21277).
‡ Present address: Department of Pharmacology, Beth Israel Hospital, Boston, MA 02215.

[1] Abbreviations: HiPIP, high-potential iron–sulfur protein, a class of [4Fe-4S] ferredoxins found in some bacteria; Tris-HCl, tris(hydroxymethyl)aminomethane hydrochloride.

0006-2960/85/0424-2542$01.50/0

Table I: HiPIP Absorption Spectral Properties and Redox Potentials

HiPIP source	$E_{m,7}$ (mV)	purity index of oxidized state ($A^{UV}_{max}/A^{vis}_{max}$)	$\epsilon_{vis,max}$ (M^{-1} cm^{-1})	$\Delta\epsilon_{500nm}$ (M^{-1} cm^{-1})
C. vinosum	356[g] (340)[h]	2.2[a]	16.1×10^3	9.3×10^3
T. roseo-persicina	342 (294)[i]	2.2[e]	14.7×10^3 [d]	8.2×10^3
C. gracile	347	2.2[e]		9.7×10^3
T. pfennigii	352[g]	2.3[b]	15.3×10^3 [b]	8.3×10^3
Rp. gelatinosa	332[g] (313)[h]	1.8[a]	15.3×10^3 [a]	8.8×10^3
Paracoccus sp.	282[g]	1.7[c]	14.8×10^3 [c]	7.0×10^3
E. vacuolata iso-2	150	2.2[e]		8.8×10^3
E. vacuolata iso-1	260	1.9[e]		8.8×10^3
E. halophila iso-2	50	2.2[e]		8.6×10^3
E. halophila iso-1	110	2.1[e]		8.6×10^3
Rs. tenue 2761	302	1.1[e]		8.4×10^3
Rs. tenue 3761	304	1.1[e]	16.9×10^3 [c]	8.4×10^3
Rp. globi-formis	453	1.8[f]		6.6×10^3

[a] Dus et al., 1967. [b] Meyer et al., 1983. [c] Bartsch, 1978. [d] Zorin & Gogotov, 1984. [e] This work. [f] Since we were unable to fully oxidize the protein, the purity index given is for the reduced oxidation state. [g] From Mizrahi et al. (1980). [h] E_m value at pH 9.0. [i] E_m value at pH 8.7.

(negative maxima at 348 and 394 nm), and of an oxidized 2[4Fe-4S] ferredoxin (positive maxima at 325 and 425 nm), structurally similar to *P. aerogenes*, was given (Carter, 1977b) as experimental support for this proposal.

Recently, the use of natural CD, as well as magnetic CD, as a nondestructive diagnostic probe of cluster type has been investigated (Stephens et al., 1978). Natural CD was found to be too sensitive to protein environmental factors to be of utility in identifying [4Fe-4S] cluster types of a given oxidation state. However, as Carter (1977b) suggests, such protein influences, observed in the visible CD, reflect the redox properties of [4Fe-4S] clusters. Thus, we have investigated the visible (as well as far- and near-UV) CD of both oxidation states of a large number of diverse HiPIP examples to determine the validity of a HiPIP CD/redox behavior correlation. The results suggest no simple, strict correlation exists between visible CD features and a given HiPIP oxidation state. The reported redox potentials for several new HiPIP examples extend the potential range for the class from approximately 50 to 450 mV. Further, we have empirically interpreted the absolute spectra and pH perturbation difference CD spectra of certain HiPIPs in terms of amino acid sequence and assumed structural homology with *C. vinosum* HiPIP and make tentative assignments of some of the observed spectral features.

Materials and Methods

HiPIPs from different sources were isolated and purified by the general procedure outlined by Bartsch (1978). Purity indexes for the oxidized state of the proteins, $\Delta\epsilon_{500nm}$ and oxidation–reduction potentials are summarized in Table I. For those HiPIPs for which previously published extinction coefficients did not exist, the $\Delta\epsilon_{500nm}$ values were estimated by one of two methods. The extinction coefficients, for HiPIPs reducible by ferrocyanide, were calculated from the $E_{m,7}$ values for the HiPIPs determined by the spectral electrochemical measurements (see below) and the absorbance changes observed in the method of mixtures experiment (see below) in a form of the Nernst equation relating the HiPIP couple to the ferricyanide/ferrocyanide couple. For those HiPIPs not appreciably reduced by ferrocyanide (HiPIPs from the *Ectothiorhodospira sps.*), the $\Delta\epsilon_{500nm}$ values were estimated from an average $\epsilon_{375nm,ox}$ (19.4×10^3 M^{-1} cm^{-1}) from *Chromatium vinosum and Rhodopseudomonas gelatinosa* HiPIPs (Dus et al., 1967) and the spectral properties of the oxidized and reduced oxidation states at 500 nm of the given protein.

All absorption spectra were taken with a Cary 118 recording spectrophotometer at ambient temperature. CD spectra were measured at ambient temperature (23–25 °C) or thermostated at 23 °C in a water-jacketed cylindrical cell. CD measurements were made on a Cary 60 with a 6001 CD attachment. Fully oxidized and fully reduced forms of all HiPIPs were obtained by titrating samples with aliquots of well-buffered concentrated stock solutions of potassium ferricyanide or sodium dithionite, respectively, or by addition of small amounts of the solid reagent. Since all HiPIPs were found to undergo to various extents slow autooxidation and/or autoreduction [cf. Adzamli et al. (1981)], an excess of redox reagent was added in order to maintain a single oxidation state during spectral acquisition. Each spectrum was rescanned at least twice, and the final spectrum shown was the average of at least two different samples. Data in the 250–600-nm region were obtained in a 10-mm cylindrical quartz cuvette. In some cases, the entire 250–600-nm region was not obtained with the same sample. In these instances, the ellipticity values between different samples in the overlapping spectral region were in reasonable agreement. In the case of suspected base-line shifts between spectra for different wavelength regions, the spectrum for the shorter wavelength was corrected to that for the longer (e.g., near-UV spectral data corrected to the visible spectrum). Data in the 210–250-nm spectral region were obtained with a 1-mm cylindrical quartz cell with absorbance in this region kept to <2.0. Spectra at pH 7 were obtained in 10 mM Tris–cacodylate, pH 7.0, buffer. HiPIP pH difference CD spectra were obtained with sodium acetate (pH 5.1) and Tris-HCl (pH 8.7); I = 61 mM. Base lines were obtained with the appropriate buffer. CD spectra were digitized by hand with a Houston Hi-Pad digitizer and were read into a Data General Nova 2 computer for further manipulations.

Oxidation–reduction midpoint potentials were obtained for most HiPIPs by two different experimental procedures. One method was the spectroelectrochemical procedure (Earl, 1981), with the mediators methylviologen and ferrocyanide being used, and for HiPIPs with redox potentials <300 mV, Fe-EDTA was added. The second procedure was the method of mixtures [see Wilson (1978) for a description]. Typically, the oxidized HiPIP was titrated aerobically with concentrated solutions of ferrocyanide. Midpoint potentials for the ferricyanide/ferrocyanide couple at the indicated pH and ionic strengths were obtained from O'Reilly (1973). The values obtained by the two methods were in reasonable agreement (±5 mV).

Results and Discussion

The four spectral groups of the comparative HiPIP CD survey presented below are based on the reduced visible (320–600 nm) spectra. The division of the spectra into groups is based on the similarity of their spectral properties as well as spatial economy and clarity of presentation. The visible wavelength range (vs. the near- or far-UV) was chosen to group the spectra since only the [4Fe-4S] cluster absorbs in this region and thus the spectra should be most similar to each

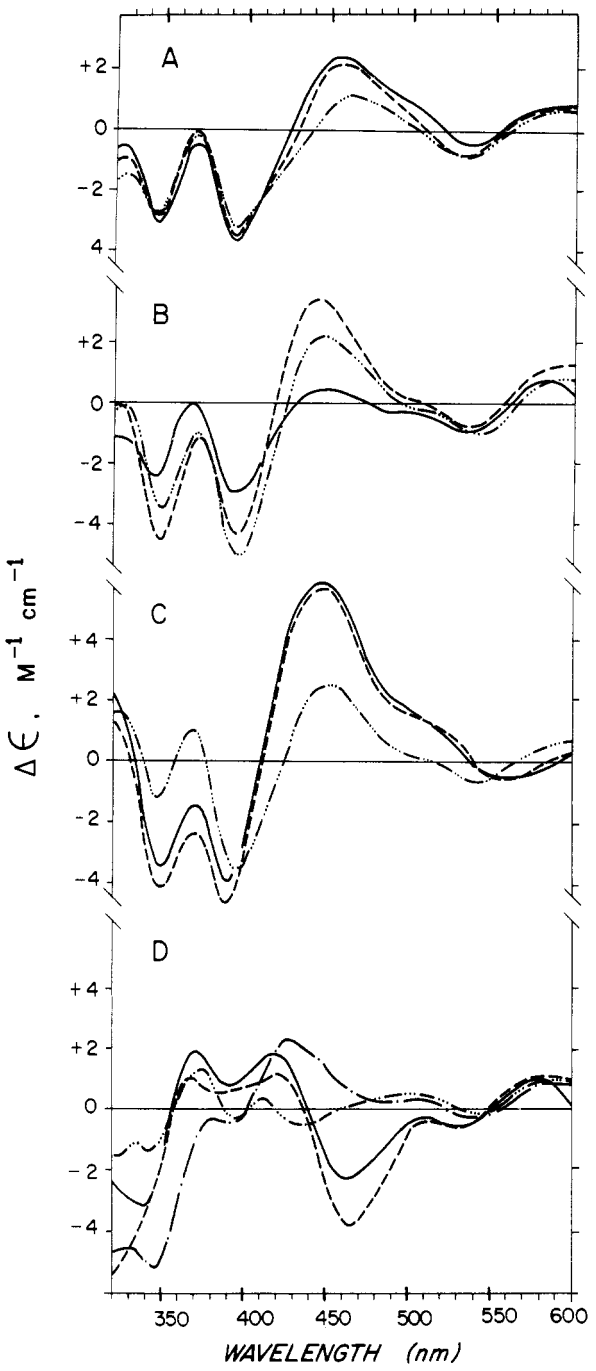

FIGURE 1: Reduced visible HiPIP CD spectra at pH 7: (group A) *C. vinosum* (—), *C. gracile* (– –), and *T. roseopersicina* (–···–); (group B) *Paracoccus* sp. (—), *E. vacuolata* iso-1 (– –), and *E. vacuolata* iso-2 (–···–); (group C) *Rp. gelatinosa* (–···–), *Rs. tenue* 3761 (—), and *Rs. tenue* 2761 (– –); (group D) *T. pfennigii* (–···–), *Rp. globiformis* (–·–), *E. halophila* iso-1 (—), and *E. halophila* iso-2 (– –).

other. Also, Carter's (1977b) prediction concerning a correlation between CD and HiPIP redox behavior, which this work examines, is based on the reduced (i.e., $[4Fe\text{-}4S]^{2+}$ cluster oxidation level) visible CD.

Visible Reduced CD Spectra. Group A (Figure 1) contains *Chromatium vinosum*, *Chromatium gracile*, and *Thiocapsa roseopersicina* HiPIPs. The similarity of their spectra is consistent with the high degree of sequence relatedness (Table II). Although group B, which contains *Paracoccus* sp. and the two iso-HiPIPs from *Ectothiorhodospira vacuolata*, could have on qualitative grounds been placed in group A, this was not done for sake of clarity of presentation. In addition, the members of this group in general have lower $E_{m,7}$ values than those of group A (Table I) and are from moderately halophilic bacteria. Group C contains the net positively charged HiPIPs (based on sequence data; Table II), *Rhodopseudomonas gelatinosa* HiPIP and the HiPIPs from two strains of *Rhodospirillum tenue*. The similarity in the two *Rs. tenue* HiPIP spectra again is consistent with the high degree of sequence relatedness between them (Table II). The group C spectra, in some respects, qualitatively resemble those of group A; however, the presence of positive ellipticity at ~330 nm warranted their placement into a separate group. Group D contains *Thiocapsa pfennigii* HiPIP, *Rhodopseudomonas globiformis* HiPIP, and the two iso-HiPIPs from *Ectothiorhodospira halophila*. These HiPIPs display the most divergent spectra from those of group A. The two iso-HiPIPs from *E. halophila*, as those from *E. vacuolata*, exhibit similar spectra. Although group D could be subdivided into additional groups, this was not done to conserve space.

The ellipticity values associated with the [4Fe-4S] cluster electronic transitions in the various HiPIPs and other [4Fe-4S]-containing ferredoxins are in general quite small in comparison to the oxidized chromophores of [2Fe-2S] ferredoxins and rubredoxins [cf. Stephens et al. (1978) and references cited therein]. This fact, coupled with the small uncertainty (estimated to be less than 10%) in some of the HiPIP extinction coefficients, may lead to errors in the magnitudes for the spectra, and therefore, for this analysis, only major qualitative differences are of significance.

As noted previously (Flatmark & Dus, 1969), the single unresolved maximum (375–388 nm; Bartsch, 1978) in the 350–600-nm region of the absorption spectrum is, on the basis of the reduced visible CD, composed of at least five to six transitions (*C. vinosum* HiPIP: negative maxima at ~347, 394, and 535 nm; positive maxima at ~456 and 590 nm with a positive shoulder at ~500 nm). The electronic origin for the major cluster visible absorption band, as well as those major transitions occuring in the near-UV (see below), has been suggested to arise from primarily S → Fe charge-transfer transitions [cf. Aizman & Case (1982)]. The geometrical cluster properties for only a single reduced HiPIP, *C. vinosum*, have been determined [cf. Carter (1977a)]. However, the observation that isoelectronic [4Fe-4S] clusters in two unrelated ferredoxins exhibit essentially identical three-dimensional structures to that of HiPIP [cf. Stout (1982) and references cited therein] suggests that the geometry of the reduced cluster in various HiPIPs is probably conserved. Thus, differences observed among the visible HiPIP CD spectra (Figure 1) are most likely due to perturbations of the cluster transitions by polypeptide interactions.

The correlation of visible CD and redox behavior proposed by Carter (1977b) is based, in part, on features of the native reduced *C. vinosum* HiPIP spectrum and that in 85% Me_2SO (pH 9.85). Specifically, the presence and magnitude of the two negative bands at 348 and 394 nm, possibly arising from Tyr-19 interactions with the cluster, were suggested to be correlated with HiPIP redox properties (Carter, 1977b). The visible CD spectrum observed for reduced *C. vinosum* HiPIP reported here (Figure 1A) is in good agreement with earlier reports (Flatmark & Dus, 1969; Hall et al., 1974; Stephens et al., 1978). A comparison of reduced spectra for other HiPIPs (Figure 1) indicates that negative maxima at approximately 350 and 400 nm are conserved in many, but apparently not all, HiPIPs. However, the model requires these features to be present in all HiPIP examples. Spectra for the HiPIPs in group D (Figure 1) indicate a dramatic alteration in these maxima, particularly in the one at ~400 nm. In

Table II: Amino Acid Sequences of High-Potential Iron–Sulfur Proteins[a]

	HiPIP source
10 20 30 40 50 60 70 80	
SAPANAVAADDATAIALKYNQDATKSERVAAARPGLPPEEQHCANCQFMQADAAGATDEWKGCQLFPGKL-INV--DGWCASWTLKAG	*C. vinosum*
EAPANAVAANDPTAVALKYNADATKSDRLAAARPGLPPAEQHCANCQFHLDDVAGATEEWHGCSLFPGKL-INV--DGWCASWTLKAG	*T. roseopersicina*
EVPANAVTESDPTAVALKYHRNAEASERVAAARPGLPPEEQHCENCQFMLPD-QGA-DEWRGCSLFPGKL-INL--DGWCASWTLRAG	*C. gracile*
EDLPHVDAATNPIAQSLHYIEDANASERNPVTKTELPGSEQFCHNCSFIQAD----SGAWRPCTLYPGYT-VSE--DGWCLSWAHKTA	*T. pfennigii*
APVD-EKNPQAVALGYVSDAAKADK-AKYKQFVAGS--HCGNCALFQGK---ATDAVGGCPLFAGKQ-VAN--KGWCSAWAKKA	*Rp. gelatinosa*
QDLPPLD-PSAEQAQALNYVKDTAEAA--DHPA-HGEGE--QCDNCMFFQAD-------SQGCQLFPQNS-VEP--QGWCQSWTAQN	*Paracoccus* sp.
GLPDGVEDLPKAEDDHAHDYVNDAADT---DHAR-FQEGQ--LCENCQFWVDYVN----GWGYCQ-HPDFTDVLVRGEGWCSVYAPA	*E. halophila* iso-2
EPRAEDGHAHDYVNEAADP---SHGR-YQEGQ--LCENCAFWGEAVQ---DGWGRCT-HPDFDEVLVKAEGWCSVYAPAS	*E. halophila* iso-1
GTNASMRKAFNY-QEVSKT----------AGK--NCANCAQFIPGAS-AS-AAGACKVIPGDSQIQP--TGYCDAYIVKK	*Rs. tenue* 3761
GTNAAMRKAFNY-QDTAK----------NGK---CSGCAQFVPGAS-PT-AAGGCKVIPGDNEIAP--GGYCDAFIVKK	*Rs. tenue* 2761

[a] Tedro et al. (1981) and S. M. Tedro, T. E. Meyer, and M. D. Kamen (unpublished results).

several group D proteins, there appear to be negative inflections superimposed on positive maxima at 400 nm, and it is possible that there is some cancellation occurring. However, *E. halophila* iso-2-HiPIP, which has been found to give an oxidized state EPR spectrum (Cammack, 1979) identical with other HiPIPs (Antanaitis & Moss, 1975; Blum et al., 1978; Sands, 1979; Zorin & Gogotov, 1984), completely lacks inflection in the 350-nm region, and it is unclear whether an inflection exists at 400 nm. We conclude that a strict correlation between utilization of the 3+/2+ [4Fe-4S] cluster oxidation levels and visible CD does not exist, but we also acknowledge that other interpretations are possible, that is, cancellation of the negative maxima by new positive bands at ~350 and ~400 nm. In the absence of any supporting data, we do not feel comfortable proposing new bands at this time (see following). *Rp. globiformis* HiPIP (group D), which has the highest redox potential of any HiPIP found to date (Table I), and the *E. vacuolata* iso-HiPIPs (group B; as compared to *C. vinosum* HiPIP) have spectra that indicate no strict, simple correlation exists between the magnitude of the negative maxima at ~350 and ~400 nm and redox potentials of proteins using the 3+/2+ [4Fe-4S] cluster oxidation levels, as was suggested by Carter (1977b). On the basis of the present alignment of amino acid sequence data, *E. halophila* iso-HiPIPs and *T. pfennigii* HiPIP (which in the context of this argument have featureless CD spectra) appear to have Tyr-19 conserved (Table II). We expect spatial conservation of Tyr-19 in *T. pfennigii* HiPIP, because it is relatively similar to *C. vinosum* HiPIP in sequence. However, it is possible that Tyr-19 is not spatially conserved in *R. tenue* HiPIP because of large sequence differences and the presence of insertions and deletions. We conclude that there is also no simple relationship between the presence of Tyr-19 and the negative maxima in CD spectra near 350 and 400 nm. Whether or not Tyr-19 occupies a structurally identical position with respect to the iron–sulfur cluster awaits verification by crystallographic studies, particularly with *R. tenue* HiPIP or a member of spectral group D.

Visible Oxidized CD Spectra. The oxidized CD spectra of the HiPIPs studied are shown in Figure 2. Our spectrum for *C. vinosum* HiPIP differs somewhat from the previously published spectra (Flatmark & Dus, 1969; Hall et al., 1974; Stephens et al., 1978). The spectrum of Flatmark & Dus (1969) has been suggested by Stephens et al. (1978) to be incorrect due to incomplete oxidation of their sample. The difference between the *C. vinosum* spectrum observed in the present study and that of Stephens et al. (1978) can probably be attributed to an undetected base-line shift in one of the

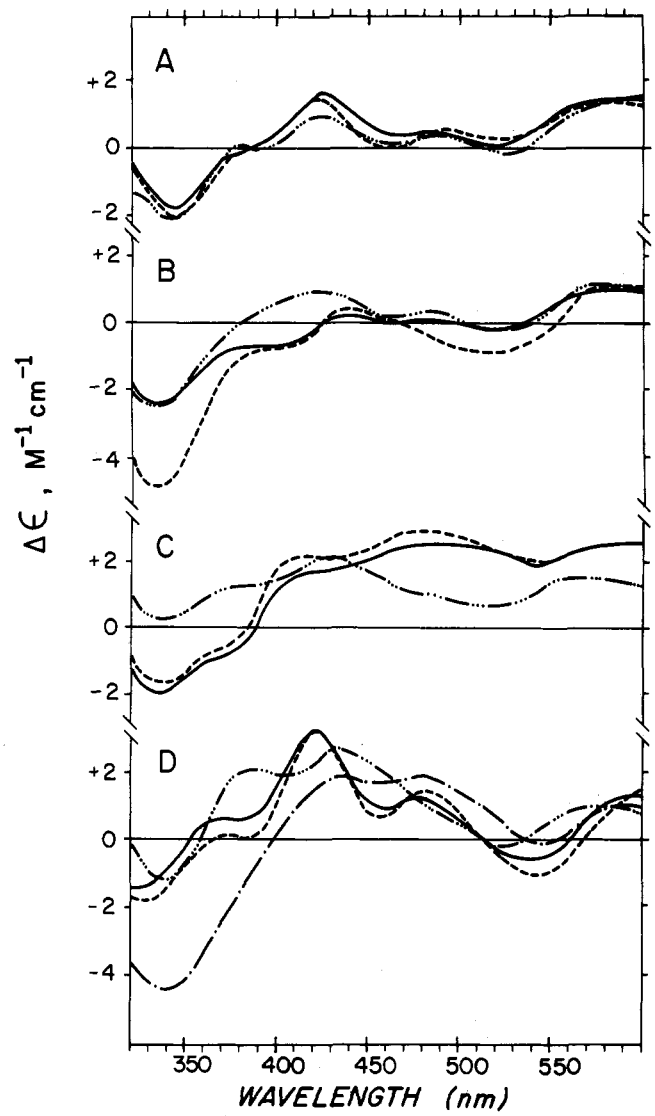

FIGURE 2: Oxidized visible HiPIP CD spectra at pH 7. Legend for spectra is as in Figure 1, except for group B: *Paracoccus* sp. (–···–), *E. vacuolata* iso-1 (—), and *E. vacuolata* iso-2 (– –).

spectra. Confidence in the qualitative correctness of the *C. vinosum* spectrum in the present study is obtained from the fact that a large number of different HiPIPs display similarly shaped oxidized spectra (Figure 2).

The oxidized visible absorption spectrum of HiPIP is rather featureless with broad maxima at approximately 320, 400, and

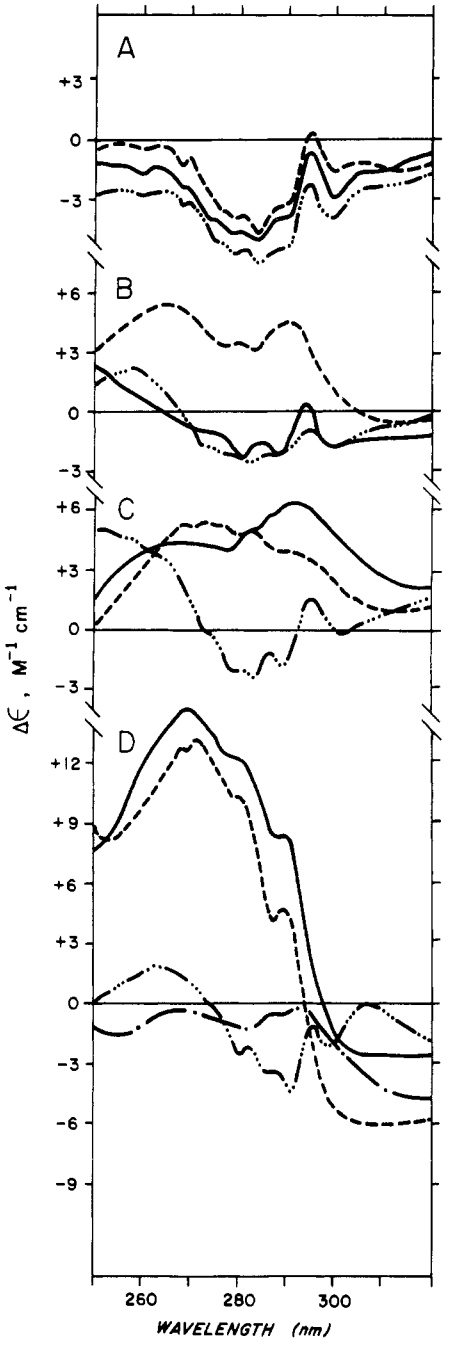

FIGURE 3: Reduced near-UV HiPIP CD spectra at pH 7. Legend to spectra is as in Figure 1.

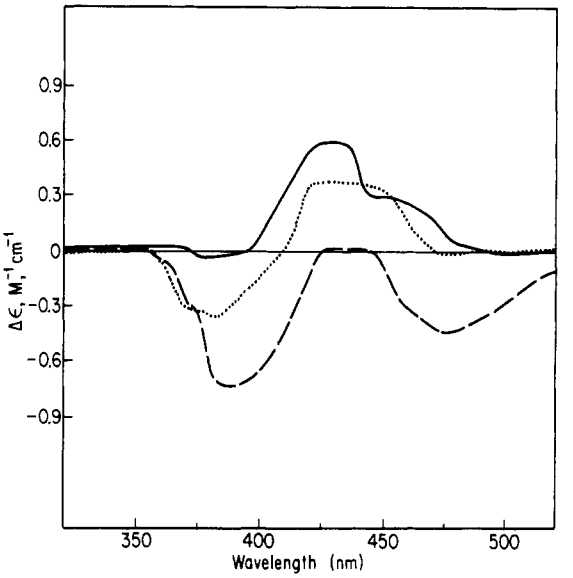

FIGURE 4: Reduced visible HiPIP pH 8.7 minus pH 5.1 difference CD spectra: *C. vinosum* (—), *Rp. gelatinosa* (···), and *T. roseopersicina* (– –). The digitized spectra were subtracted by computer.

450 nm (Bartsch, 1978). The oxidized *C. vinosum* HiPIP CD spectrum exhibits a negative maximum at ~346 nm and three positive maxima at 425, 488, and 580 nm. HiPIP spectra in groups B–D appear to possess a negative maximum in the 320–350-nm region (*Rp. gelatinosa* being an exception) and in general display many spectral features in common with the spectra in group A. The apparently greater similarity of the oxidized visible spectra (vs. the reduced state) among the different HiPIPs may result from differences in the cluster electronic or geometrical structure between the two oxidation states and/or the fewer polypeptide interactions that can occur as a result of the proposed cluster contraction that occurs upon oxidation [cf. Carter (1977b)].

Near-UV Reduced CD Spectra. In addition to the cluster absorbance [maximum ~280–300 nm; cf. Aizman & Case (1982)], HiPIPs have aromatic amino acids that contribute to the absorbance in the near-UV wavelength region (250–320 nm; Figure 3). Thus, the CD in this region is quite complicated. The fact that the spectra differ in sign as well as magnitude suggests that extensive cancellation effects may be occurring.

In *C. vinosum* HiPIP, X-ray crystallographic studies have shown that all but one (Trp-60) of the aromatic residues (Tyr-19, Phe-48, Phe-66, Trp-76, and Trp-80) within the protein are packed in close proximity (<5 Å) to atoms of the cluster. Thus, it is probable that many of the aromatic residues and cluster transitions are strongly coupled to one another. The vibronic fine structure associated with aromatic side-chain CD [cf. Strickland (1974)] is apparent in the HiPIP near-UV spectra (Figure 3). For example, a 290-nm peak characteristic of tryptophan is generally present. For HiPIPs with similar aromatic residue composition and sequence positions, qualitatively similar spectra are observed (cf. group A, Figure 3 and Table II). From an examination of the various HiPIP sequences, the presence of a negative shoulder at ~290 nm appears to be associated with Trp-80, on the basis of the current sequence alignment (*Chromatium* numbering). HiPIPs that do not possess this spectral feature (*Rp. globiformis*, *E. vacuolata* iso-1, *Rs. tenue* 3761 and 2761, and the *E. halophila* iso-HiPIPs) do not have Trp-80 [Table II; S. M. Tedro, T. E. Meyer, and M. D. Kamen (unpublished results) and R. P. Ambler, T. E. Meyer, U. Fischer, and M. D. Kamen (unpublished results)]. It is interesting that the *E. halophila* iso-HiPIPs display a *positive* shoulder at ~290 nm. The single additional Trp residue in these HiPIPs, not found in the other HiPIPs, is Trp-49. Consistent with the possible involvement of this residue in this apparently enantiomeric spectral feature is the fact that, assuming structural homology with *C. vinosum* HiPIP, Trp-49 approaches the cluster from the opposite side of the effective mirror plane as compared to Trp-80 (Carter, 1977b), assuming that the same face of the tryptophan mirror plane faces the iron–sulfur cluster.

pH Perturbations of HiPIP Visible CD. The importance of interactions of amino acid side-chain residues at positions 49 and 80 with the cluster, as suggested above, receives some support from the observation that *T. roseopersicina* HiPIP, which has a histidine at position 49 (Table II), demonstrates a relatively strong pH dependence on its oxidation–reduction potential (see Table I). *C. vinosum* and *Rp. gelatinosa* Hi-

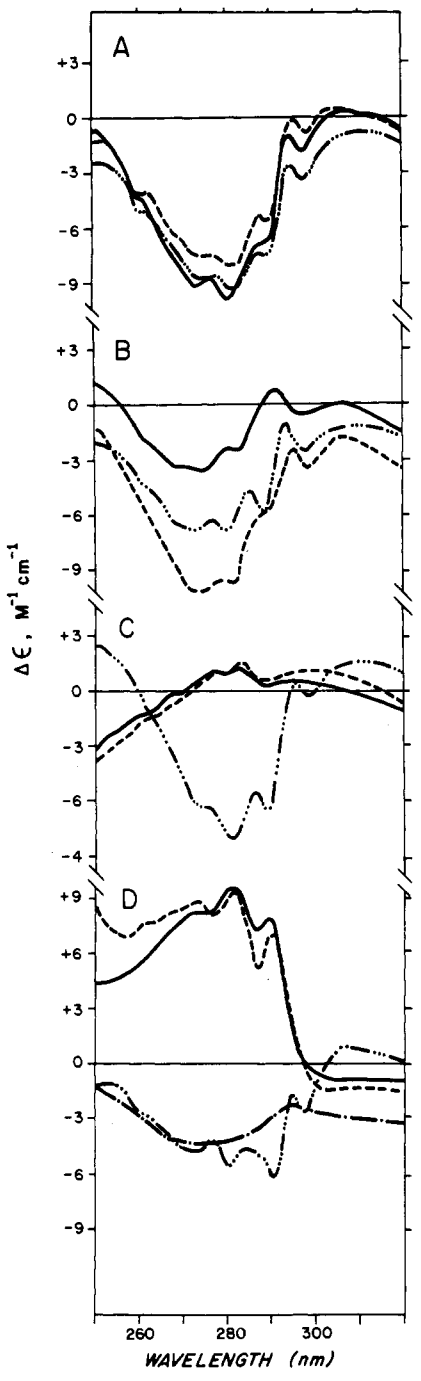

FIGURE 5: Oxidized near-UV HiPIP CD spectra at pH 7. Legend for spectra is as given in Figure 1.

PIPs, which both have histidine at position 42, have a smaller change in midpoint potential (Table I). Since *T. roseopersicina* HiPIP has another histidine (His-61) besides His-49, not found in common with *C. vinosum*, one cannot unequivocally assign the pH effects observed with *T. roseopersicina* to His-49. However, on the basis of the *C. vinosum* HiPIP structure, His-61 is further removed from the cluster than His-49 (which would be located within 5 Å of the S_4^* atom of the cluster, assuming homology to *C. vinosum* HiPIP).

The effect of pH on redox potential is consistent with an electrostatic interaction of the protonated form of a histidine residue with the negatively charged cluster, as has been previously suggested for the sole His-42 in *C. vinosum* and *Rp. gelatinosa* HiPIPs (Nettesheim et al., 1983). A small pH difference CD spectrum in the reduced form is observed for *T. roseopersicina* HiPIP, which is different from those ob-

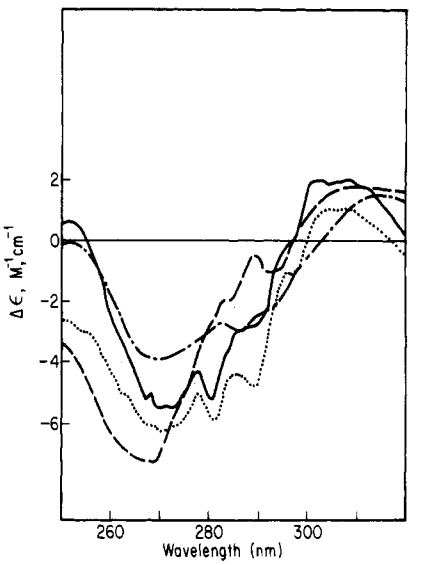

FIGURE 6: Oxidized minus reduced HiPIP near-UV difference CD: *C. vinosum* (—), *Rp. gelatinosa* (···), *Rp. globiformis* (–·–), and *E. halophila* iso-1 (– –). Digitized spectra from Figure 3 were subtracted from digitized spectra in Figure 5.

served for *Rp. gelatinosa* and *C. vinosum* HiPIPs (Figure 4). The reduced oxidation state was studied, since, if an electrostatic interaction is involved, it would be expected to demonstrate a larger effect than with the oxidized state because of the more negative cluster charge. Further, support for the interpretation that the CD difference spectra are due to histidine ionization is obtained from the fact that reduced *Rs. tenue* 3761 HiPIP, which contains no histidine (Table II), produces no pH-induced CD difference spectrum. Thus, protonation of His (42 or 49) appears to result in a pH-induced CD difference spectrum as well as a change in midpoint potential.

Near-UV Oxidized CD Spectra. As in the reduced state, aromatic vibronic structure is also apparent in the oxidized near-UV CD spectra (Figure 5). The correlation between the negative shoulder at ~290 nm and Trp-80 (see above) is maintained in the oxidized state. As suggested by Flatmark & Dus (1969), the cluster probably accounts for a major portion of the differences observed between the near-UV spectra for the two oxidation states. The general similarity of the oxidized minus reduced difference CD spectra for HiPIPs, which demonstrate drastically different absolute CD spectra, supports this proposal (Figure 6). The additional differences observed between the spectra in Figure 5 are apparently due to differences in the aromatic residue contributions.

Far-UV Reduced CD Spectra. The far-UV spectral region (210–250 nm) is characterized by contributions due not only to various amino acid side chains, and presumably the [4Fe-4S] cluster, but also the peptide bond [cf. Brahams & Brahams (1980)]. In instances where the protein has little secondary structure, especially α-helix, aromatic side chains are suggested to make important contributions to this wavelength region (Woody, 1978; Brahams & Brahams, 1980). On the basis of the X-ray crystallographic studies of *C. vinosum* HiPIP, which suggest only ~12% of polypeptide chain is in an α-helical conformation, such a situation would be expected to apply to HiPIP. The negative band at ~230 nm in the *C. vinosum* spectrum (Figure 7) is similar in position to bands previously attributed to aromatic side chains (tyrosine and tryptophan; Woody, 1978). Again, the group A HiPIPs display, as expected, very similar spectra in this region. It was

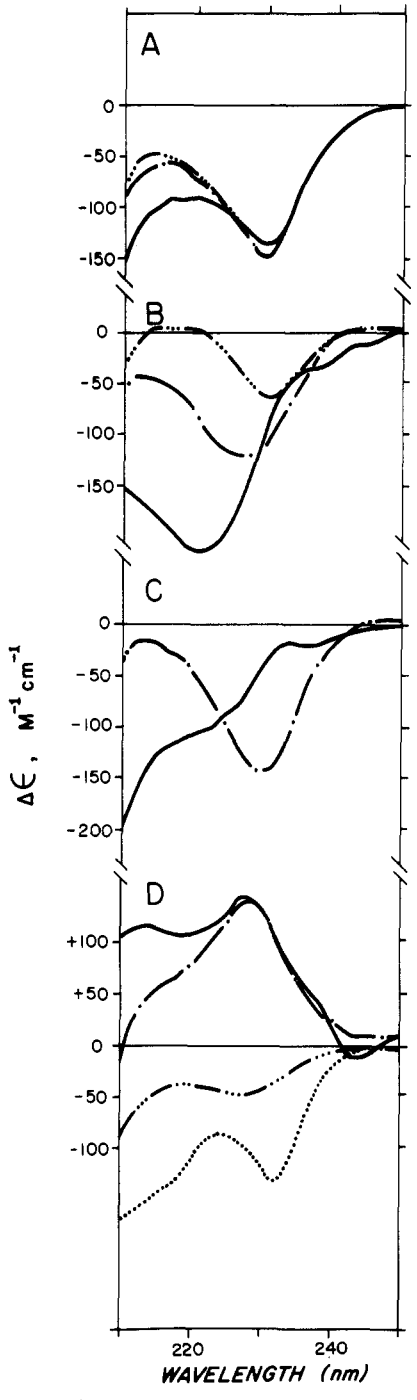

FIGURE 7: Reduced far-UV HiPIP CD spectra at pH 7: (group A) *C. vinosum* (—), *C. gracile* (– –), and *T. roseopersicina* (–···–); (group B) *Paracoccus* sp. (–···–), *E. vacuolata* iso-1 (—), and *E. vacuolata* iso-2 (–·–); (group C) *Rp. gelatinosa* (–·–) and *Rs. tenue* 3761 (—); (group D) *T. pfennigii* (···), *Rp. globiformis* (–···–), *E. halophila* iso-1 (—), and *E. halophila* iso-2 (–·–).

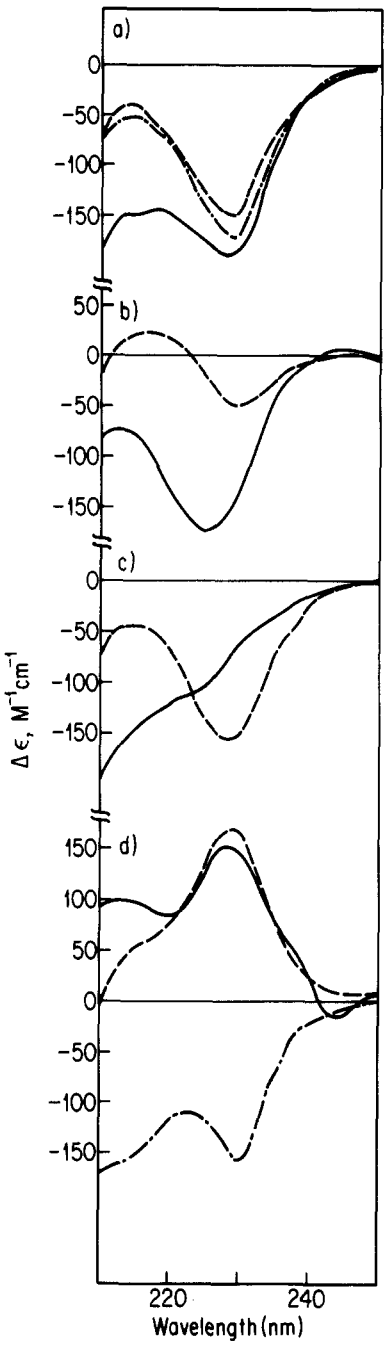

FIGURE 8: Oxidized far-UV HiPIP CD spectra at pH 7: (group A) *C. vinosum* (—), *C. gracile* (– –), and *T. roseopersicina* (–·–); (group B) *Paracoccus* sp. (– –) and *E. vacuolata* iso-2 (—); (group C) *Rp. gelatinosa* (– –) and *Rs. tenue* 3761 (—); (group D) *T. pfennigii* (–·–), *E. halophila* iso-1 (—), and *E. halophila* iso-2 (– –).

previously suggested that the 230-nm band was associated with the cysteinyl coordination of the cluster (Flatmark & Dus, 1969); however, the finding that several HiPIPs do not possess this band (Figure 7) argues against this proposal and in favor of the predominant involvement of aromatic residues. Significantly, the *E. halophila* iso-HiPIPs (group D) again display an approximately enantiomeric relationship to the group A spectra with regard to the band at ~230 nm. This may result in part from Trp-49 with the negative maxima in other HiPIPs being attributed in part to Trp-80. The apparent absence of prominent negative maxima at ~230 nm in the *Rs. tenue*, *Rp. globiformis*, and *E. vacuolata* iso-1 HiPIPs supports this speculation. All the CD spectra indicate little or no α-helix content, consistent with the *C. vinosum* crystal structure (12% helix) (Carter et al., 1974a).

Far-UV Oxidized CD Spectra. The oxidized-state far-UV spectra demonstrate some differences from the reduced state for all HiPIPs (Figure 8). For *C. vinosum* HiPIP, the maximum at ~230 nm shifts to ~228 nm, increasing slightly in intensity. There are also some small changes at shorter wavelengths. These changes can probably be attributed to cluster oxidation-state differences and/or aromatic residue environment effects [cf. Nettesheim et al. (1980)]. Crystallographic studies have indicated only small conformational changes between the oxidized and reduced states of *C. vinosum* HiPIP (Carter et al., 1974b).

Conclusions

No strict, simple correlation appears to exist between reduced visible CD features and the utilization of the 3+/2+ oxidation levels of the iron–sulfur cluster in HiPIP as was suggested by Carter (1977b). There is also no apparent correlation between CD properties and oxidation–reduction potentials or presence of Tyr-19. However, certain amino acid side chains in close contact to the cluster appear to be important in modifying spectral and oxidation–reduction properties. Specifically, the negative shoulder at ~290 nm and the negative maximum at ~230 nm are apparently associated with the presence of Trp-80. In *E. halophila* iso-HiPIPs, which do not possess a Trp-80, the positive bands at ~290 and ~230 nm appear to be associated with Trp-49, which is located on the opposite side of the effective mirror plane of the cluster from Trp-80. The possible importance of position 49 due to its proximity to the iron–sulfur cluster is supported by the influence of pH on the redox potential and visible CD properties of *T. roseopersicina* HiPIP, which has a histidine at position 49.

The data presented here cannot be interpreted quantitatively until more detailed assignments of the bands arising from the iron–sulfur cluster are available and the spectra are deconvoluted. Nevertheless, by comparison of the spectra of a wide variety of homologous proteins we are able to make tentative assignments of a number of major transitions (far-UV, near-UV, and vis) as well as address the proposals of Carter (1977b). Moreover, the general similarity of CD spectra for HiPIPs with a wide range of oxidation–reduction potentials and in some cases little amino acid sequence similarity establishes the structural homology within this class of iron–sulfur proteins.

References

Adzamli, I. K., Davies, D. M., Stanely, C. S., & Sykes, A. G. (1981) *J. Am. Chem. Soc. 103*, 5543–5542.

Aizman, A., & Case, D. A. (1982) *J. Am. Chem. Soc. 104*, 3269–3279.

Antanaitis, B. C., & Moss, T. H. (1975) *Biochim. Biophys. Acta 405*, 262–279.

Bartsch, R. G. (1978) *Methods Enzymol. 53*, 329–340.

Blum, H., Salerno, J. C., & Cusanovich, M. A. (1976) *Biochem. Biophys. Res. Commun. 84*, 1125–1128.

Brahams, S., & Brahams, J. (1980) *J. Mol. Biol. 138*, 149–178.

Cammack, R. (1973) *Biochem. Biophys. Res. Commun. 54*, 548–554.

Cammack, R. (1979) *Abstract of Papers*, International Congress of Biochemistry, 11th, Toronto, Canada, National Research Council of Canada, Ottawa, Canada.

Carter, C. W., Jr. (1977a) in *Iron-Sulfur Proteins* (Lovenberg, W., Ed.) Vol. 3, pp 157–204, Academic Press, New York.

Carter, C. W., Jr. (1977b) *J. Biol. Chem. 252*, 7802–7811.

Carter, C. W., Jr., Kraut, J., Freer, S. T., Alden, R. A., Sieker, L. C., Adman, E. T., & Jensen, L. H. (1972) *Proc. Natl. Acad. Sci. U.S.A. 69*, 3526–3529.

Carter, C. W., Jr., Kraut, J., Freer, S. T., & Alden, R. A. (1974a) *J. Biol. Chem. 249*, 6339–6346.

Carter, C. W., Jr., Kraut, J., Freer, S. T., Xuong, N. H., Alden, R. A., & Bartsch, R. G. (1974b) *J. Biol. Chem. 249*, 4212–4225.

Dus, K., DeKlerk, H., Sletten, K., & Bartsch, R. G. (1967) *Biochim. Biophys. Acta 140*, 291–311.

Earl, R. A. (1981) Ph.D. Dissertation, University of Arizona, Tucson, AZ.

Flatmark, T., & Dus, K. (1969) *Biochim. Biophys. Acta 180*, 377–387.

Fukumori, Y., & Yamanaka, T. (1979) *Curr. Microbiol. 3*, 117–120.

Hall, D. O., Cammack, R., & Rao, K. K. (1974) *Iron in Biochemistry and Medicine* (Jacob, A., & Worwood, M., Eds.) pp 249–334, Academic Press, London.

Herskovitz, T., Averill, B. A., Holm, R. H., Ibers, J. A., Phillips, W. D., & Weiher, J. F. (1972) *Proc. Natl. Acad. Sci. U.S.A. 69*, 2437–2441.

Meyer, T. E., Przysiecki, C. T., Watkins, J. A., Bhattacharyya, A., Simondsen, R. P., Cusanovich, M. A., & Tollin, G. (1983) *Proc. Natl. Acad. Sci. U.S.A. 80*, 6740–6744.

Mizrahi, I. A., Meyer, T. E., & Cusanovich, M. A. (1980) *Biochemistry 19*, 4727–4733.

Nettesheim, D. G., Meyer, T. E., Feinberg, B. A., & Otovs, J. D. (1983) *J. Biol. Chem. 258*, 8235–8239.

O'Reilly, J. E. (1973) *Biochim. Biophys. Acta 292*, 509–515.

Sands, R. H. (1979) in *Multiple Electron Resonance Spectroscopy* (Dorio, M. M., & Freed, J. H., Eds.) pp 331–374, Plenum Press, New York.

Stephens, P. J., Thomson, A. J., Dunn, J. B. R., Keiderling, T. A., Rawlings, J., Rao, K. K., & Hall, D. O. (1978) *Biochemistry 17*, 4770–4778.

Stombaugh, K. D., Sundquist, J. E., Burris, R. H., & Orme-Johnson, W. H. (1976) *Biochemistry 15*, 2633–2641.

Stout, C. D. (1982) in *Iron-Sulfur Proteins* (Spiro, T. G., Ed.) pp 97–146, Wiley, New York.

Strickland, E. H. (1974) *CRC Crit. Rev. Biochem. 2*, 113–175.

Sweeney, W. V., & Rabinowitz, J. C. (1980) *Annu. Rev. Biochem. 49*, 139–161.

Tedro, S. M., Meyer, T. E., Bartsch, R. G., & Kamen, M. D. (1981) *J. Biol. Chem. 25*, 731–735.

Wilson, G. S. (1978) *Methods Enzymol. 54E*, 396–410.

Woody, R. W. (1978) *Biopolymers 17*, 1451–1467.

Zorin, N. A., & Gogotov, I. N. (1984) *Biochemistry* (*Engl. Transl.*) *48*, 1011–1016.